Available online at www.sciencedirect.com

ScienceDirect

IFAC PapersOnline CONFERENCE PAPER ARCHIVE

IFAC PapersOnLine 51-22 (2018) 298–305

Fast Iterative 3D Mapping for Large-Scale Outdoor Environments with Local Minima Escape Mechanism

Haris Balta * **Jasmin Velagic** ** **Walter Bosschaerts** *
Geert De Cubber * **Bruno Siciliano** ***

* *Royal Military Academy, Department of Mechanics, Brussels, Belgium, (e-mail: haris.balta@rma.ac.be).*
** *Department of Automatic Control and Electronics, Faculty of Electrical Engineering, Sarajevo, Bosnia and Herzegovina, (e-mail: jasmin.velagic@etf.unsa.ba)*
*** *Department of Electrical Engineering and Information Technology, University of Naples Federico II, Napoli, Italy, (e-mail: bruno.siciliano@unina.it)*

Abstract: This paper introduces a novel iterative 3D mapping framework for large scale natural terrain and complex environments. The framework is based on an Iterative-Closest-Point (ICP) algorithm and an iterative error minimization mechanism, allowing robust 3D map registration. This was accomplished by performing pairwise scan registrations without any prior known pose estimation information and taking into account the measurement uncertainties due to the 6D coordinates (translation and rotation) deviations in the acquired scans. Since the ICP algorithm does not guarantee to escape from local minima during the mapping, new algorithms for the local minima estimation and local minima escape process were proposed. The proposed framework is validated using large scale field test data sets. The experimental results were compared with those of standard, generalized and non-linear ICP registration methods and the performance evaluation is presented, showing improved performance of the proposed 3D mapping framework.

Keywords: Unmanned ground vehicle, outlier removal, 3D point cloud, large-scale environment, FCSOR.

1. INTRODUCTION

In recent years, the applications of autonomous robot systems have been migrating from indoor to outdoor environments. The high complexity of outdoor environments poses a special challenge for existing autonomous robotic technologies, especially for robots performing the desired tasks without continuous human guidance. Fully autonomous exploration and 3D mapping of rough terrain and unstructured environments impose the robot's capability to reason about the characteristics of the outdoor environment. One of the main challenges of such a task is the optimal and timely fusion of 3D data in order to improve the perception capabilities and the scene understanding.

In order to successfully navigate through rough unstructured terrain, the autonomous robotic system needs produce a precise 3D reconstructed map of the complex environment and to provide good mobility. Our paper is focused on 3D model reconstruction based on the point cloud representation. The point clouds are used by the 3D perception systems as an basic input data in order to represent the scanned environment. In order to extract useful information from the point clouds it is first necessary to process and register the individual 3D scans into a global representation. One of the main requirements of the 3D map reconstruction is to match different consecutive data measurements in order to estimate the changes in the pose between these two measurements. The output of the pose estimation is a transformation matrix representing the rotation and translation.

In our paper, the matching and displacement estimation of two consecutive point cloud measurements is solved by using a novel framework based on an improved Iterative-Closest-Point (ICP) method allowing fast and accurate registration of 3D environmental models. The proposed framework, named Local Minima Escape ICP (LME-ICP), is hierarchically organized into a multi-level processing schema. It does not require any prior known pose estimation information acquired from sensing systems like odometry, global positioning system (GPS) or inertial measurement units (IMU). The main improvements of the existing ICP algorithm lie in the estimation of the local minima situations for the new environmental scan and a novel mechanism for a local minimum escape. These provide a good matching accuracy and an optimal registration process for the 3D map building. The advantage of this approach is the ability to deal with large-scale outdoor environment data sets, while providing a fast registration, map building and a precise pose estimation. An additional component within the framework has the ability to estimate the local minima and escape from them.

10.1016/j.ifacol.2018.11.558

2. RELATED WORK

In this section, we present an overview of related work on 3D map reconstruction. The goal of a 3D map registration process is to estimate the transformation parameters between two partially overlapping scans. 3D mapping of an unstructured outdoor environments is currently a very popular research topic. Research is carried out using different type of mapping strategies and algorithms, as presented in (Zhang et al. (2011)). Additionally, considerable effort has been introduced for finding suitable sensor systems for such 3D mapping tasks (Mobedi and Nejat (2012)). In (Rattar and Sammut (2015)), the authors use an active stereo vision camera and a laser rangefinder for building a 3D map of the environment. In (Thrun et al. (2004)), two orthogonal 2D laser rangefinders are used to reconstruct 3D maps of indoor and outdoor environments, while authors in (Nuchter et al. (2005)) use 2D range finders mounted on a tilt unit that is able to acquire a very precise 3D scan of the environment.

Depending on the methodology for assessing the initial displacement, 3D registration algorithms may be categorized into two main groups: feature-based and featureless methods. For feature-based registration methods (Stamos and Leordeanu (2003), Mian et al. (2010)), the theoretical framework is well developed and it applies predefined offline geometric shape descriptors. These descriptors values are used as features to find correspondences between two 3D scans. The major advantage of using a feature-based approach over a featureless methodology is the possibility to reduce the dimensionality of the search space. Consequently, irrelevant points such as outliers have no direct effect on the 3D registration process. An additional advantage is that the registration process is not directly dependent on the initial alignment of the scans. Nevertheless, feature-based approaches are suffering from a high computational complexity. Moreover, the performance of the registration is directly dependent on the process of finding distinct features which are common in both scans. These facts may impose limitations on using this approach on large scale outdoor environments.

In contrast to the feature-based approach, the featureless approach can be applied to unstructured outdoors environments, where finding distinct features is an challenging task. One of the commonly used featureless registration approaches is the iterative closest point (ICP) algorithm introduced in (Besl and McKay (1992)). The ICP algorithm is mainly used for 3D object reconstruction and 3D mapping. The ICP algorithm takes as input two 3D scans (point clouds) $\boldsymbol{M}_{model}$ and $\boldsymbol{P}_{source}$ and tries to iteratively update the transformation $\boldsymbol{T}$ in order to minimize the distance (error) between the two data scans. One data scan is fixed, while the estimated transformation is applied on the second one in order to match the reference. The transformation parameters are estimated by using closed-form solutions as presented in (Lorusso et al. (1995)). ICP approaches can use multiple different existing registration techniques, like point-to-point, point-to-plane, or point-to-projection techniques.

However, for any type of the registration technique, when there is a weak overlap between the two data scans, a probable convergence to the local minima is impossible to avoid. This is true because of the gradient descent based optimization procedure which can not guarantee an global optimal solution. It is obvious that in a local minimum situation, the registration of the data scans does not correspond to a good alignment. A possible approach for solving the local minima in such a situation would be an effective initial estimation (e.g. odometry of the robot) of the transformation. However, in realistic operating conditions, it is not an easy task to guarantee that an initial estimation is a good one especially when we are dealing with unstructured outdoor environments. There are some efforts of solving the local minima problem, as proposed in (Yang et al. (2013)) with a global optima ICP (Go-ICP) solution. This method combines the ICP with a branch-and-bound (BnB) scheme to obtain the optimal solution. However, due to the high computational requirements this method is not very useful for large-scale outdoor environment data sets.

Ensuring that our proposed framework is performing its desired mapping task without any pose information was important due to the specific constraints of the operational missions of this research work in the domains of search and rescue and humanitarian demining. In such application scenarios, working conditions include GPS-denied environments with magnetic interference due to strong magnetic fields coming from the mobile robot platform and from collapsed buildings. Moreover, only tracked vehicles can be used, implying that the precision of odometry is drastically compromised. In section 3, we present this novel 3D mapping framework with its main characteristics and capabilities.

3. PROPOSED 3D MODEL REGISTRATION AND MAP BUILDING FRAMEWORK

The proposed novel 3D model registration framework, which is based on the local minima estimation and the local minima escape (LME-ICP) method, is illustrated in Fig. 1. The 3D model registration schema introduces the following four-step process: data handling and preparation, ICP fine alignment, local minima estimation and local minima escape.

These processes are described in the rest of this section.

3.1 Data Handling and Preparation

The data handling and preparation module includes noise reduction through filtering and downsampling for input datasets (point clouds). It provides outliers analysis and removal, and gets more unified dense datasets, thereby saving computational and memory resources in further processing steps. The output of this framework is the filtered point cloud. More details about this are given in (Balta et al. (2018)).

3.2 ICP Fine Alignment

The ICP registration approach is one of the most popular registration method for unorganized 3D data sets (Besl and McKay (1992)). The algorithm is based on an iterative gradient descent method which estimates the optimal transformation between two adjacent 3D scans using a

Euclidean distance error between their overlapping areas. The ICP method used in our paper is given in more details in (Pomerleau et al. (2015)).

3.3 Local Minima Estimation

Due to the open loop and iterative nature of the ICP algorithm, it is not possible to guarantee the avoidance of local minima. Additional drawbacks of the ICP approach are a small convergence domain and the requirement for a high number of iteration steps until convergence is reached. If the ICP algorithm gets trapped into a local minimum, this leads to erroneous estimations which can be far away from a global optimal solution. Most usual cases where the ICP algorithm fails are poor initial alignment of the data scans and additional noise coming from the unstructured outdoor environments. A possible approach for solving the local minima in such a situation would be providing a good initial estimation of the transformation. However, it is not an easy task to guarantee that the initial estimation is good, especially when dealing with harsh environments. Because of that, our proposed 3D mapping framework does not rely on any prior known pose estimation information (like odometry, GPS, IMU). In order to overcome situations where the estimation transformation of the 3D registration method is far from a global optimal solution we have introduced an error evaluation mechanism to perceive the local minimum situation. Using this mechanism we define a cost function which represents the mean of the squared Euclidean distance between corresponding points of the source $\boldsymbol{P}_{source} = \{\boldsymbol{p}_i\}$, and the reference $\boldsymbol{M}_{model} = \{\boldsymbol{m}_i\}$, datasets, where $i = 1, \ldots, N_r$.

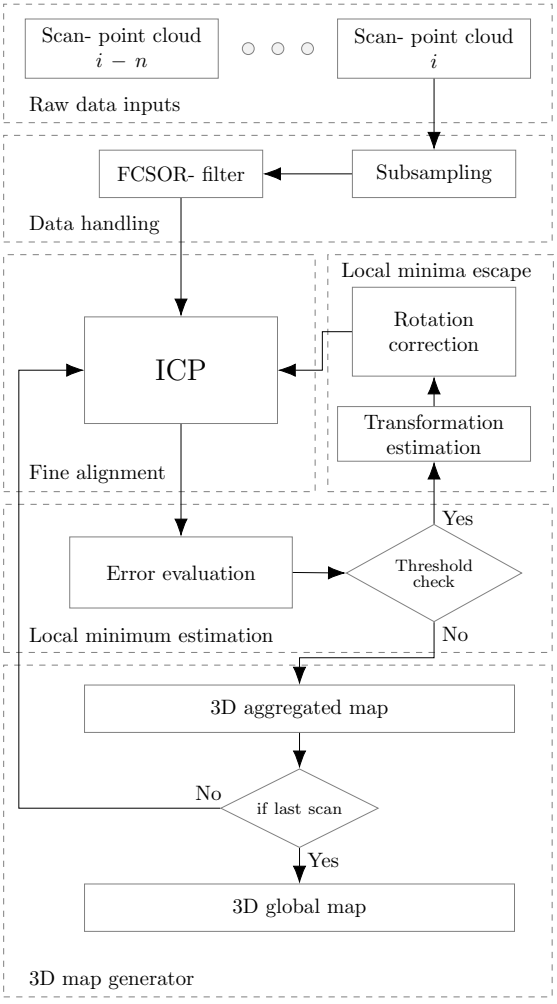

Fig. 1. Novel 3D model registration framework scheme.

The mean square error e function is defined as:

$$e = \frac{\sum_{i=1}^{N_r} \| \boldsymbol{m}_i - \boldsymbol{p}_i \|^2}{N_r} \quad (1)$$

where $\boldsymbol{m}_i$ and $\boldsymbol{p}_i$ represent the nearest corresponding points between the reference and source dataset, respectively. The corresponding pair points are found by utilizing the K - d tree nearest neighbour search algorithm (Klasing et al. (2009)). Using the distance measure between the corresponding pair points ($\boldsymbol{m}_i$, $\boldsymbol{p}_i$), we can calculate the mean squared error between the scans. Each new scan will incrementally increase the global map by adding new environmental information. Some of the new points will not have corresponding overlapping points in the global map and they introduce a large distance error. In order to get a better error estimation, we calculate the pair of corresponding points ($\boldsymbol{m}_i$, $\boldsymbol{p}_i$) only in an overlapping area which is defined within a certain radius r.

An example of such situation is shown in Fig. 2. Two successive scans are presented with the blue and red point clouds. The overlapping area contains a subsite of N_r points between the two scans. In the Fig. 2 the overlapping area is represented by the green colored points, with a number of $N_r = 24$ points in total. In this case, the overlap radius is taken as a fixed value of r between two points and the error estimation is computed. As already mentioned, defining a radius is necessary in order to avoid error accumulation of points which represent new data of the global map.

By tracking the error we can determine if the matching has achieved an accurate registration result or it has been trapped into a local minimum. Fig. 3 shows a situation where the system has detected a local minimum situation. In this figure we can see a sudden change in angle of rotation of the position of the scan (90 degrees) which is indicated with the blue scan. In this case the error has significantly increased and the system is trapped into the local minima.

Evaluating the error we can usually anticipate that a higher value of the error means that the registration processes has reached a local minimum situation, while a lower value indicates that the registration is successful. However, due to sensor noise a perfect registration is usually not possible to obtain. Therefore we need to define a threshold value in order to evaluate the computed error. If the evaluated error is below a given threshold (which is empirically evaluated using scan evaluation and is usually between 0.5 and 0.7) the alignment is good and the new scan can be merged into the global map. If not, the local minima escape mechanism will be activated.

3.4 Local Minima Escape

If the new scan was trapped in a local minimum as shown in Fig. 3, a new transformation is computed which is going

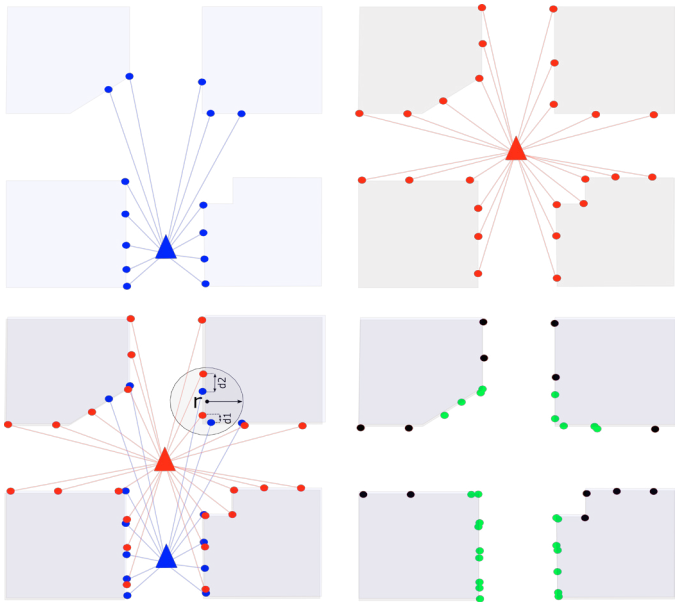

Fig. 2. Scan registration sequence, upper left and right illustrations are showing two successive scans, left lower figure is showing the overlapping area with the error estimation in certain radius r, right lower figure shows registred scan where green points representing the overlapping points and the black point are the new added point from the second scan (red).

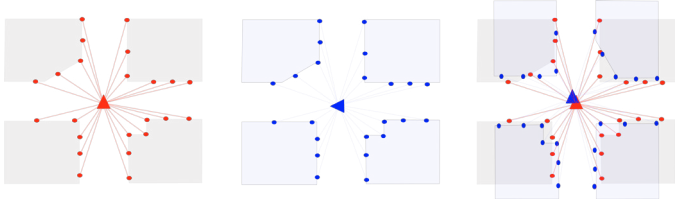

Fig. 3. Local minima situation caused by an significant change of the angle of rotation.

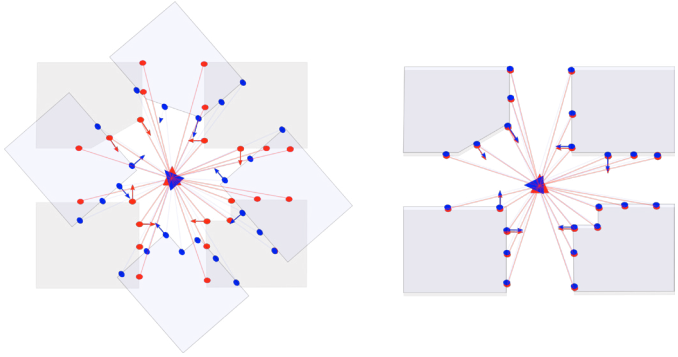

Fig. 4. Local minima escape, computation of surface normals and two step local minima escape.

to move the scan out of the local minimum situation. First, we find all the overlapping points between the global map and the new scan by utilizing the nearest neighbor search (Segal et al. (2009),Bentley (1975)). In the second step the surface normals (Klasing et al. (2009)) are computed on the new scan point cloud and overlapping points from the global map as shown in Fig. 4.

This gives an additional robustness to the transformation as we take in consideration the type of surfaces. For example points from a wall will be matched only to other points in a wall and so on. The surface normals are directly estimated from the point cloud dataset. The general idea of estimating the normal to a point on the surface is approximated by the normal estimation of a plane tangent to the surface. In general this becomes a least-square plane fitting estimation problem. This computation can be done by calculating the covariance matrices of the points and then extracting the eigenvalues and eigenvectors. By analyzing the eigenvalues and eigenvectors we can define the surface normals of a point. Pseudocode representation of the implemented surface normal estimation is presented in the (Klasing et al. (2009)).

After the surface normal estimation, we extract pairs of points form the new scan and overlapping points from the map which have similar normals. After the pairs of points with similar normals have been extracted from the new scan and global map, a rigid transformation between the pairs is computed. With this transformation, we are able to bring the new scan closer to the global map and avoid the local minima. An additional step has been added to improve the transformation efficiency. Because most of the matched pairs come from around the center of the new scan, the new transformation will be close to the local minima. Therefore, we avoid using these points all together. As a result, the new transformation places the new scan further away from the local minima (Algorithm 1).

The experimental verification of the proposed 3D model registration framework is given in the next section.

4. EXPERIMENTAL RESULTS AND COMPARATIVE ANALYSIS

In order to provide required perceptual data input for environmental perception and navigation assistance, a depth sensing system was integrated on the UGV (RMA tEODor UGV). This exteroceptive 3D mapping system is dedicated to gathering 3D data of the mission environment. The RMA tEODor UGV (Fig. 5) has excellent maneuverability over the rough terrains and good off-road performance through its tracked system. During the mapping process the RMA tEODor UGV usually traverses 4 - 5 m between

Algorithm 1 Pseudocode representation of the local minima escape process

INPUT : New 3D data scan and global map: $\boldsymbol{P}_{source} = \{\boldsymbol{p}_j\}$, $\boldsymbol{M}_{model} = \{\boldsymbol{m}_i\}$, Nearest points in $\boldsymbol{M} \rightarrow \boldsymbol{P}$

OUTPUT: The correct transformation, $\boldsymbol{T}$, which aligns $\boldsymbol{M}_{model}$ and $\boldsymbol{P}_{source}$

if *error* > *thrashError* **then**
  Find nearest points in $\boldsymbol{M}$ with points in $\boldsymbol{P}$ [*excluding points near the center*] $\rightarrow \boldsymbol{K}$;
  Calculate normals for point clouds $\boldsymbol{P}$ and $\boldsymbol{K}$;
  Find pairs of points from $\boldsymbol{P}$ and $\boldsymbol{K}$ with similar normals $\rightarrow \boldsymbol{P}_s$ and $\boldsymbol{K}_s$;
  Find rigid transformation between $\boldsymbol{P}_s$ and $\boldsymbol{K}_s \rightarrow \boldsymbol{T}$;

end

each scan. The distance between scans is one of the key parameters in the mapping framework. Because this allows a good overlap between the scans. For each scan of the environment the laser scanner needs to perform a full revolution which usually takes around 10 sec. Afterwards the iterative 3D mapping framework is applied performing point cloud registration, where the latest scan is localized and matched to previous scans increasing the overall 3D map of the environment. The process is repeated until a complete 3D map is constructed.

In order to assess the proposed 3D mapping framework, we have used an accurate geodetic reference model of the scanned area created by an terrestrial geodetic laser system Z+F IMAGER 5010 and registered with geodetic precision. Due to the high precision and accuracy (1 mm) of the geodetic reference model, we were able to use it as ground truth in order to compare it with the generated model by our 3D mapping framework. Moreover, we have performed a qualitative and quantitative evaluation of our proposed LME-ICP method in presence of the local minima in acquired scans by adding additional translational and rotational errors. The computation time and CPU occupancy for the reconstruction of the 3D global map from acquired scans were analysed and a comparative analysis between three state of the art ICP registration methods and our proposed 3D mapping framework was also elaborated. In all cases we have used the least square method, which is extensively used in regression analysis and estimation, to compare the obtained final results.

The experimental setup presented here was carried out at the Camp Roi Albert, one of the largest military bases of the Belgian Defence (locateMarche-en-Famenne, Belgium). Our proposed method will be compared with three concurrent methods: Standard ICP, Generalized ICP, Non-linear ICP. For the first evaluation step, we have analyzed the convergence of our proposed mapping framework and the three other ICP methods for a scan-by-scan registration approach using as an input two random successive scans. After the scan-by-scan evaluation, a global map registration analysis was performed. In this step we have evaluated the complete dataset for both experiments while taking the performance evaluation as well as the matching accuracy in order to generate a complete and consistent model. In the last section of the results, we have presented the ground truth data evaluation, were the global maps registered by our 3D mapping framework have been compared with respect to a reference model ground truth data calculated with high-accuracy geodetic precision.

Fig. 5. RMA tEODor UGV with the 3D mapping hardware.

4.1 Scan-by-Scan Convergence Evaluation

In this subsection a rigorous testing procedure was performed with respect to coordinate errors between two consecutive scans. The error we introduced was randomly generated within the values of respective x, y, z Cartesian coordinates $e_t \in [-10\,m, +10\,m]$ for the translation error and for the rotational error the φ, θ, ψ (roll, pitch, yaw) angles were produced within the values of $e_r \in [-75°, +75°]$ for each axis respectively. These generated errors are significantly larger than the real ones and impose more extensive and strict demands for testing procedures of the effectiveness and robustness of the methods.

Fig. 6 shows the registration results of around 40 transformation error test on the rubble field scenario. As an indicator for the quality of the method, both the average translation and rotation errors were employed. Even by introducing large errors, our proposed 3D mapping framework was able to guarantee exceptional matching accuracy, while the other methods produced significant errors caused by failure to escape from local minima.

In the considered scenario, the average rotational and translational errors obtained by applying the proposed LME-ICP method are respectively 0.05° and 0.1 m. In comparison to the other three considered methods, these errors are at least 30 times smaller for the translational component and at least 380 times smaller for the rotational component of the error. Too larger translational and rotational errors of the other methods between two consecutive scans are the result of the absence of the local minima escape mechanism.

To clearly demonstrate the superiority of our proposed method the additional evaluation parameters are used. These parameters are translation errors about respective coordinate axes x, y, z, average translational error μ_T and variance of translational error σ_T^2. The same parameters

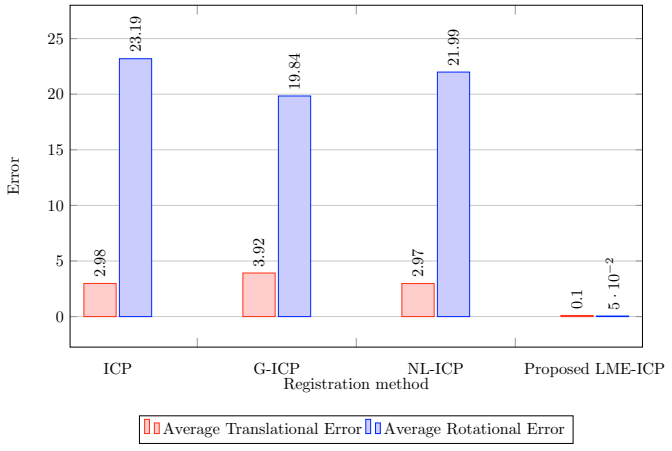

Fig. 6. Quantitative results of the average error for the Standard ICP, Generalized ICP, Non-linear ICP and our proposed LMI-ICP method for the Rubble field scenario

are considered for the rotational error ϕ, θ, ψ. Table 1 gives an analytical representation of the registration results with introduced transformation error for translational and rotational components of the registration methods. The obtained results additionally confirm the superiority the proposed method in comparison to the other three considered methods. This means that the values of the all parameters are noticeably smaller in the case when our method is applied.

Table 1. Analytical representation of the results

Dataset Rubble					
Method	Translational Error [m]				
	x	y	z	μ_T	σ_T^2
ICP	4.09	3.07	1.76	2.98	6.67
G-ICP	6.14	3.56	2.06	3.92	11.83
NL-ICP	4.18	3.03	1.68	2.97	6.63
LME-ICP	0.21	0.07	0.01	0.10	0.20
Method	Rotation Error [deg]				
	ϕ	θ	ψ	μ_R	σ_R^2
ICP	14.60	14.82	40.16	23.19	378.76
G-ICP	10.65	14.22	34.66	19.84	423.61
NL-ICP	11.62	14.41	39.94	21.99	317.18
LME-ICP	0.04	0.06	0.05	0.05	0.02

Table 2 shows the error where 90 % of the point which are within the given distance. For our proposed LME-ICP method, we have an average error of around 0.17 m, allowing us to generate a consistent model of the environment.

Table 2. Point to Point Evaluation

90% of the points are within the distance of	Rubble field scenario
ICP	0.55 m
G-ICP	0.55 m
NL-ICP	0.59 m
LME-ICP	0.17 m

4.2 Global Map Evaluation

In this subsection, the results of performance analysis, as well as the qualitative comparison of the reconstructed maps are given. In order to evaluate the ability of the local minima escape process, several indicators are used: the computation time (time of execution - ToE), the quality of the global map reconstruction (Average matching error - AME) and the required computer resources (Average CPU load - ACP) for the completion of the specified task. For each scenario, we acquired number of scans (NoS) more than 90 for the global map reconstruction (in our scenario 95). The computational time is the time needed for the reconstruction of the complete global map. Furthermore, the number of local minima (NLM) and escape from local minima (ELM) are also determined.

The obtained results shown in Table 3 indicate that the proposed method generates the global map of the rubble field 7 - 9 times faster than G-ICP and NL-ICP. In comparison with the ICP method, our method is a bit slower in terms of the computation time, as it requires some time to perform the local minima escape process. However, the ICP method is not able to consistently reconstruct the global map due to the fact that that it has no local minima escape mechanism, as well as other considered ICP-based methods. It is important to note that our method simultaneously satisfies both desired capabilities: the ability to reconstruct a consistent and accurate global map and the possibility to generate the global map within a satisfactory time interval. The proposed method successfully escapes from the local minima and it requires approximately 13.39 seconds. In terms of CPU load needed for the global map reconstruction, the smallest CPU effort is needed for ICP method.

Table 3. Performance analysis for the Dataset Rubble.

Dataset RUBBLE					
Method	ToE(s)	ACP(%)	NLM	ELM	AME(m)
ICP	243.07	25.18	5	failed	0.28
G-ICP	3179.32	26.19	68	failed	0.52
NL-ICP	2138.27	27.25	13	failed	0.32
LME-ICP	340.44	27.03	9	9	0.27

The resulting reconstructed global maps using the considered ICP methods are shown in Figs.7a - d.

These ICP-based methods generate inconsistent and poor global maps due to lacking of the local minima escape. On the contrary, the proposed LME-ICP method produces a comprehensive map fulfilling the necessary requirements to accurately match all the scans. Producing these good results was directly linked to the problem of the local minima escape which was the main contribution of this paper. The real environment and the scanning trajectory of the robot is shown in the Fig. 8.

The obtained robot global map trajectories for all considered methods are shown in Fig. 9. Trajectories obtained by using concurrent ICP based methods are inconsistent which are a direct consequence of their poor local minima escape capabilities, whereas our proposed method is capable to reconstruct the 3D environmental model from the acquired scans.

The time needed for the global 3D map reconstruction with respect to the number of scans, using the considered methods, is shown in Fig. 10. The G-ICP and NL-ICP methods spent much more time in processing of data for map reconstruction from the scans than the ICP and the proposed LME-ICP methods. The ICP method required less time in comparison to our method, but it has no ability to generate consistent 3D global map. Our proposed

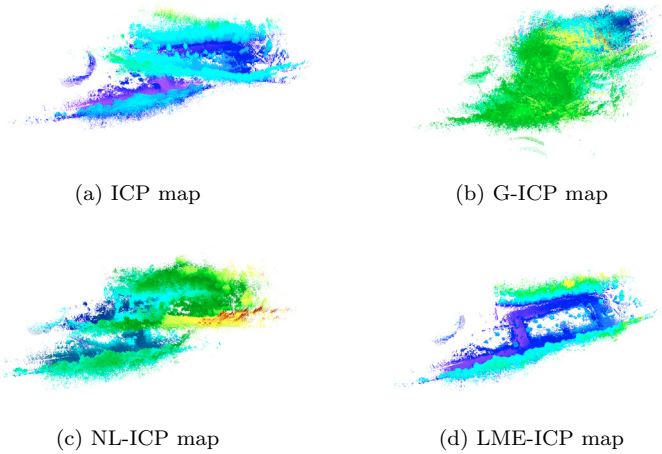

(a) ICP map (b) G-ICP map

(c) NL-ICP map (d) LME-ICP map

Fig. 7. Reconstructed global maps.

Fig. 8. Real environment :: Rubble field scenario

method successfully escapes from the local minima in the average time of 13.39 seconds.

In order to estimate the deviation of the other considered methods from the proposed LME-ICP method, we have calculated the Euclidian distance between corresponding robot positions each scan. The obtained results, given in Table 4, list the average Euclidian distance for all three methods. From these results, it can be concluded that the coordinate deviation is significant in all three cases, especially in the case of G-ICP method.

Table 4. Trajectory Error Analysis dataset Rubble

Registration Method	Average Euclidian Distance (m)
ICP	8.62
G-ICP	47.22
NL-ICP	15.09

4.3 Ground Truth Data Evaluation

For evaluation the global maps registered by our 3D mapping framework, we have used as reference model ground truth data measured with high accuracy geodetic precision. Ground truthing was performed in collaboration with the IMM institute (Bedkowski et al. (2014)). We compared the data reconstructed using our 3D mapping framework with respect to the ground truth using the least square method. The comparison of the maps generated by our 3D mapping framework and the ground truth data is shown in Fig. 11.

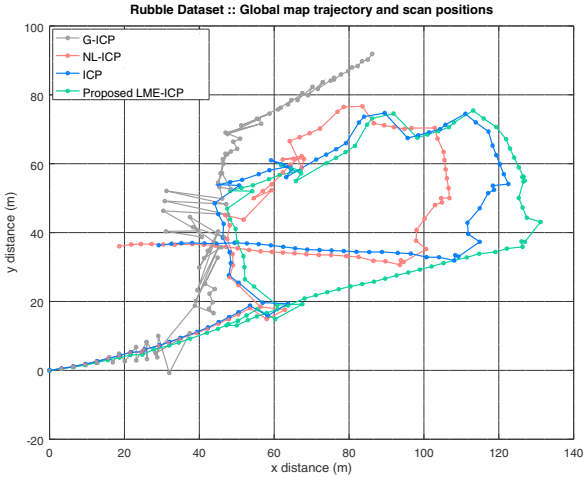

Fig. 9. Trajectory for all considered methods.

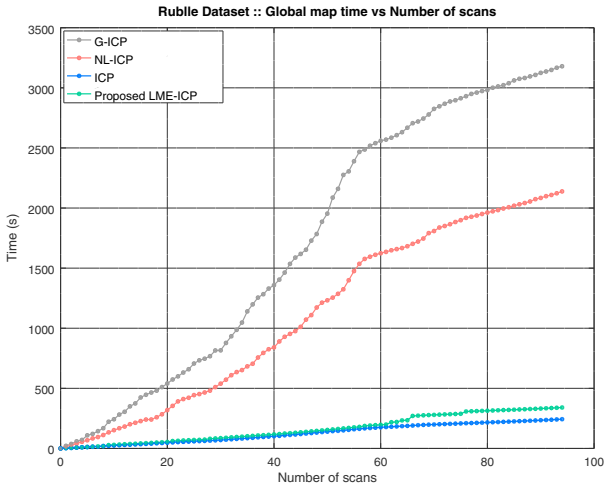

Fig. 10. Reconstruction time for all methods

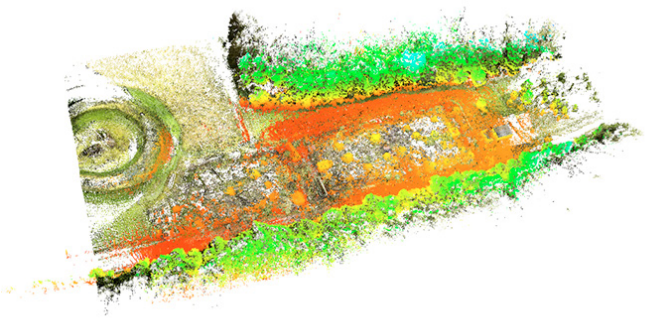

Fig. 11. Comparison of the reference ground truth model (multi-colored) and resulting maps of our proposed mapping framework (gradient-green-red) for the rubble field scenario. Dataset: Military-base Marcheen-Famenne, Belgium.

In order to compare other ICP methods with respect to the ground truth reference model, the point to point histograms of the point distribution with respect to their distances are calculated. The obtained point to point histograms are shown in the Fig. 12. Table 5 shows the error, were 90 % of the point which are within the given distance.

Table 5. Point to Point Evaluation

90% of points within given distance	Rubble field scenario
ICP	0.88 m
G-ICP	0.89 m
NL-ICP	0.86 m
Proposed LME-ICP	0.53 m

5. CONCLUSIONS

A novel iterative 3D mapping framework for large-scale natural terrain and complex environments has been proposed in this paper. The main parts of this framework are the local minima estimation and the local minima escape mechanism. The novel framework, entitled LME-ICP, is introduced to enforce the standard ICP method

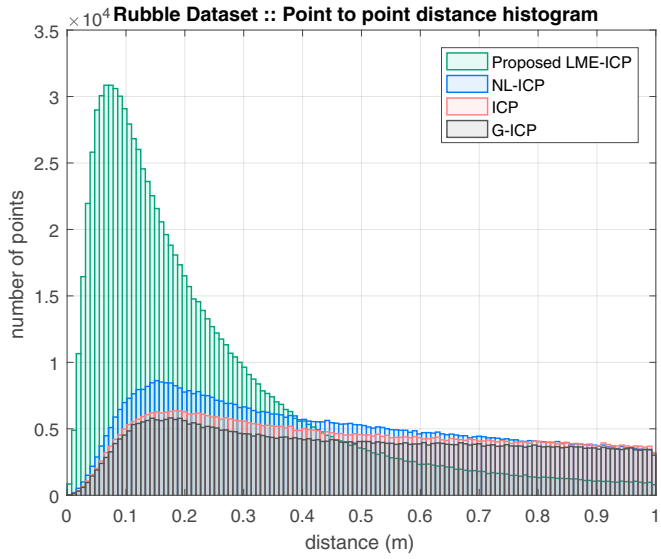

Fig. 12. Point to point error histograms calculated by the distances between points from the ground truth reference model and the maps generated by our proposed 3D mapping framework.

in order to escape from identified local minima. The proposed framework is validated using a large scale field data sets. The experimental results were compared with those of standard, non-linear and generalized ICP registration methods. Moreover, we have validated our framework with reference model ground truth data calculated with high accuracy geodetic precision. The results and performance evaluation are presented, showing excellent performance of the proposed framework.

REFERENCES

Zhang, Z., Nejat, G., Guo, H. and Huang, P. (2011). A novel 3d sensory system for robot-assisted mapping of cluttered urban search and rescue environments. *Intelligent Service Robotics*, volume 4, pages 119–134.

Mobedi, B. and Nejat, G. (2012) 3-d active sensing in time-critical urban search and rescue missions. *IEEE/ASME Transactions on Mechatronics*, volume 17, pages 1111–1119.

Ratter, A. and Sammut, C. (2015). Fused 2D/3D position tracking for robust SLAM on mobile robots. IEEE/RSJ International Conference on Intelligent Robots and Systems, September 28 - October 2, Hamburg, Germany, pages 1962–1969.

Thrun, S., Martin, C., Liu, Y., Hahnel, D., Emery-Montemerlo, R., Chakrabarti, D. and Burgard, W. (2004). A real-time expectation maximization algorithm for acquiring multi-planar maps of indoor environments with mobile robots. *IEEE Transactions on Robotics and Automation*, volume 20, pages 433–443.

Nuchter, A., Lingemann, K., Hertzberg, J. and Surmann, H. (2005). 6D SLAM with approximate data association. International Conference on Advanced Robotics, April 18-22, Seattle, USA, pages 242–249.

Stamos, I. and Leordeanu, M. (2003). Automated feature-based range registration of urban scenes of large scale. IEEE Computer Society Conference on Computer Vision and Pattern Recognition, Madison, USA, pages 555–561.

Mian, A., Bennamoun, M. and Owens, R. (2010). On the repeatability and quality of keypoints for local feature-based 3D object retrieval from cluttered scenes. *International Journal of Computer Vision*, volume 89, pages 348–361.

Besl, P. and McKay, N.D. (1992). A method for registration of 3D shapes. *IEEE Transactions on Pattern Analysis and Machine Intelligence*, volume 14, pages 239–256.

Lorusso, A., Eggert, D.W. and Fisher, R.B. (1995). A comparison of four algorithms for estimating 3-D rigid transformations. British Conference on Machine Vision, September 11-14, Birmingham, UK, pages 237–246.

Yang, J., Li, H. and Jia, Y. (2013). Go-ICP: solving 3D registration efficiently and globally optimally. IEEE International Conference on Computer Vision, 1-8 December, Sydney, Australia, pages 1457–1464.

Balta, H., Velagić, J., De Cubber, G., Bosschaerts, W. and Siciliano, B. (2018). Fast statistical outlier removal based method for large 3D point clouds of rough terrains traversal by UGV. IFAC Symposium on Robot Control, August 27-30, Budapest, Hungary, (submitted to).

Pomerleau, F., Colas, F. and Siegwart, R. (2015). A Review of point cloud registration algorithms for mobile robotics. *Foundations and Trends in Robotics*, volume 4, pages 1-104.

Klasing, K., Althoff, D., Wollherr, D. and Buss, M. (2009). Comparison of surface normal estimation methods for range sensing applications. IEEE International Conference on Robotics and Automation, Kobe, Japan, pages 3206–3211.

Segal, A., Haehnel, D. and Thrun, S. (2009). Generalized-ICP. Proceedings of Robotics: Science and Systems, Seattle, USA, 2009, pages 1–8,

Bentley, J.L. (1975). Multidimensional binary search trees used for associative searching. *ACM Communication*, volume 18, pages 509–517.

Bedkowski, J., Majek, K, Musialik, P., Adamek, A., Andrzejewski, D., Czekaj, D. (2014). Towards terrestrial 3D data registration improved by parallel programming and evaluated with geodetic precision. *Automation in Construction*, volume 47, pages 78–91.